Arsenic δ-doped HgTe/HgCdTe superlattices grown by molecular beam epitaxy

G. K. O. Tsen,[1,a)] C. A. Musca,[1] J. M. Dell,[1] J. Antoszewski,[1] L. Faraone,[1] and C. R. Becker[2]
[1]*School of EECE, The University of Western Australia, Crawley, Western Australia 6009, Australia*
[2]*Physikalisches Institut der Universitat Wuerzburg, Wuerzburg 97070, Germany*

(Received 21 December 2007; accepted 7 February 2008; published online 28 February 2008)

Arsenic incorporation in $HgTe/Hg_{0.05}Cd_{0.95}Te$ superlattices grown by molecular beam epitaxy (MBE) is reported. The incorporation was carried out by a δ-doping approach where arsenic was incorporated during MBE growth as acceptors. The superlattices were characterized via high resolution x-ray diffraction, Fourier transform infrared spectroscopy, secondary ion mass spectrometry, and magnetotransport Hall measurements coupled with the quantitative mobility spectrum analysis algorithm. © *2008 American Institute of Physics*. [DOI: 10.1063/1.2888967]

Mercury cadmium telluride (HgCdTe) is an important material in the area of infrared detection. At present, the preferred growth method for HgCdTe is molecular beam epitaxy (MBE) due to the controllable growth rate achievable and the low growth temperatures required for Hg based structures that require sharp interfaces. For achieving higher performance, fabricated infrared detectors are normally operated in the photovoltaic mode which requires a stable and reproducible technology in terms of extrinsic doping of the material during growth. While extrinsic *n*-type doping using indium and/or iodine during MBE growth is now a routine process, to date, there has not been a consistent *in situ* MBE *p*-type doping technique with the exception of that for *p*-type HgTe/HgCdTe(001) quantum wells.[1]

Out of the many *p*-type dopants available, arsenic has been the most extensively studied due to its low diffusivity in HgCdTe. However, under optimum MBE growth conditions, incorporated arsenic tends to reside on the cation sublattice sites which result in as-grown material having *n*-type characteristics. Arsenic activation then requires a high temperature postgrowth anneal to move arsenic to the anion sublattice sites where they act as *p*-type dopants. This high temperature annealing step is undesirable as defects may be introduced which prove detrimental to detector performance. The use of superlattices in this work aims primarily to alleviate the problem of achieving *in situ* low doped MBE *p*-type material while utilizing the superlattices' advantage of greater control of cutoff wavelength, higher quantum efficiency, and higher absorption coefficient. The importance of low doping in the absorber region of a detector lies in lower thermal generation and higher quantum efficiency which essentially determines the optimum performance of Auger limited detectors.[2] In this work, arsenic is incorporated in a HgTe/HgCdTe superlattice configuration during MBE growth by means of a δ-doping approach. Similar technique has previously been undertaken by Jung *et al.*[3]

The HgTe/HgCdTe superlattices were grown epitaxially on CdZnTe (211)B substrates in a Riber 2300 MBE system using source materials consisting of solid CdTe, Te, Cd_3As_2, and liquid Hg. A fixed substrate temperature of 180 °C was employed. Growth rates ranging between 2.5–3 Å/s were used for the CdTe and HgTe growth. The superlattice structure used for arsenic δ-doping of CdTe is shown in Fig. 1. The technique involves arsenic being incorporated into CdTe layers of the superlattice during growth interruptions specifically when the Te and CdTe shutters are closed. The key aspect utilized here for effective arsenic incorporation is due to the excess of mercury ions present, hence enhancing the arsenic-mercury bond formation which increases the probability of arsenic incorporation on Te sites. Furthermore, the use of a Cd_3As_2 cell source has previously been shown to minimize Hg vacancies and promote efficient *p*-type doping.[4]

Figure 2 shows the x-ray diffraction pattern for the superlattice utilizing a Bragg reflection of (224) measured in a four crystal x-ray diffractometer. The full width half maximum for the substrate and superlattice was determined to be 31 and 97 arc sec, respectively, typical values for material grown under similar conditions. From the angular separation between the main peak and the satellite peaks, a dynamic simulation of the diffraction pattern reveals a superlattice period (i.e., $d_{CdTe}+d_{HgTe}$) of about 11.8 nm.

Fourier transform infrared transmission (FTIR) optical measurements were performed on the sample at 300 K to determine the cutoff wavelength. The absorption coefficient, $\alpha(E)$ is extracted by fitting the experimental transmission data to a theoretical description of the multilayer system via

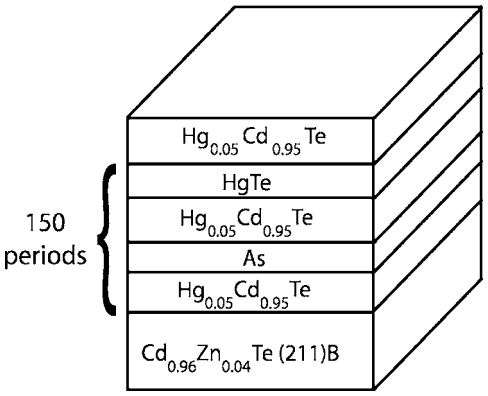

FIG. 1. Schematic of a δ-doped superlattice. The HgCdTe layers in the superlattice have the composition $Hg_{0.05}Cd_{0.95}Te$ due to the Hg cell being constantly open during the MBE growth process.

a)Electronic mail: gtko@ee.uwa.edu.au.

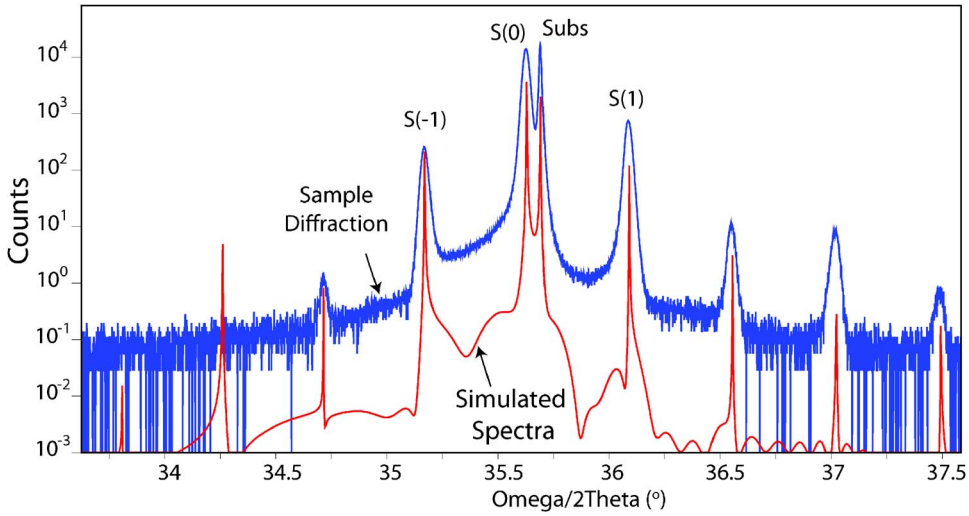

FIG. 2. (Color online) X-ray diffraction of a δ-doped superlattice with a dynamic simulation of the peaks.

a transfer matrix method. The theoretical absorption spectra and hence the intersubband transition energies are obtained by means of $k \cdot p$ band structure calculations in the envelope function approximation using the full 8×8 Kane Hamiltonian.[5] Using the well thickness d_{HgTe} as a fitting parameter, the calculated theoretical absorption coefficient spectra and experimental spectra are shown (Fig. 3). As expected, the fit is generally not as good at higher energies due to the perturbation theory involved and, as such, only the two intersubband transitions at the lower energies are used to determine the fitting. The barrier thickness d_{CdTe} is obtained from the difference between the superlattice period and the well thickness. For the sample Q2235, a barrier and well thickness of 6.4 and 5.4 nm, respectively, was calculated, which resulted in a cutoff wavelength of ≈ 10.5 μm at 300 K.

Detailed secondary ion mass spectroscopy (SIMS) analysis was carried out to determine the amount of arsenic present in the superlattice. A depth profile of iodine was also carried out as a background check as it was commonly used as an n-type dopant in prior growths (Fig. 4). For this particular sample, from the SIMS measurements, it appears that the amount of iodine and arsenic in the sample are fairly similarly low doped in the mid to high 10^{15} s cm^{-3}.

To determine the carrier type, concentration, and mobilities in the sample, Hall measurements were taken at varying temperatures at magnetic fields up to 12 T. The measurements were made on an eight-contact Hall Bar fabricated photolithographically from a standard mesa etch where Cr/Au (50/2000 Å) metal was thermally evaporated onto the contact areas. The raw resistivity and hall voltages obtained from the measurements were used as inputs to the quantitative mobility spectrum analysis (QMSA) software. QMSA is a quantitative multi carrier fitting algorithm that requires no *a priori* assumptions regarding the number and nature of carriers present in the material. Extensive analysis of the QMSA outputs may be found in Ref. 6. Figs. 5(a) and 5(b) show the carrier concentrations and mobilities extracted from QMSA as a function of temperature. Two main carriers (electron and hole) contributing to conductivity of the material were observed. At 77 K, the carrier concentrations of hole and electron were found to be 3.1×10^{15} and 1.6×10^{15} cm^{-3} with mobilities 1680 and 64 000 cm^2/V s, re-

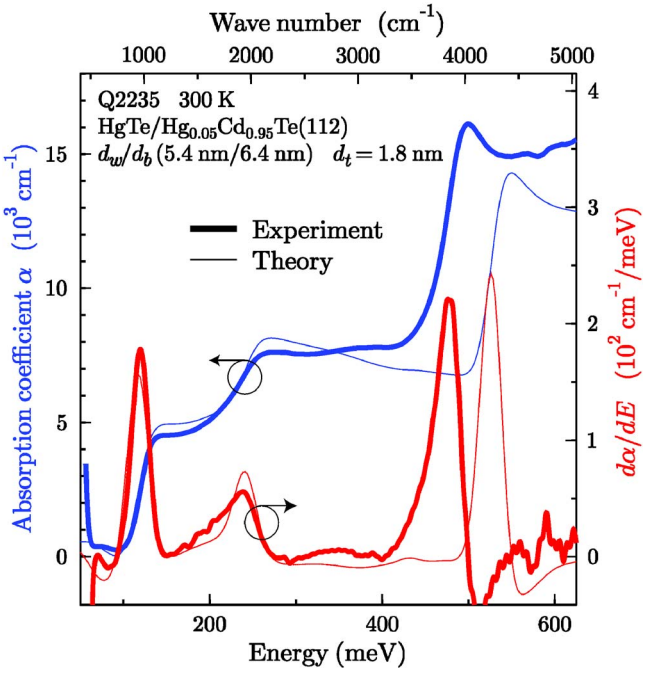

FIG. 3. (Color online) Absorption spectra of a δ-doped superlattice. The extracted cutoff wavelength at 300 K is measured to be about 10.5 μm.

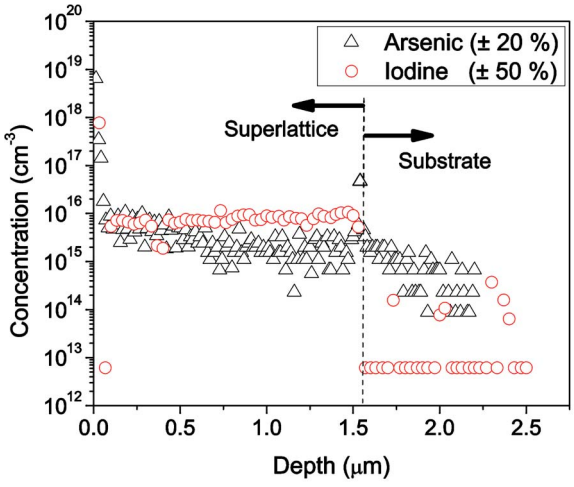

FIG. 4. (Color online) SIMS measurement on the superlattice, Q2235 indicating the presence of arsenic and iodine. The confidence levels in the SIMS measurement as quoted by Evans Analytical are also indicated.

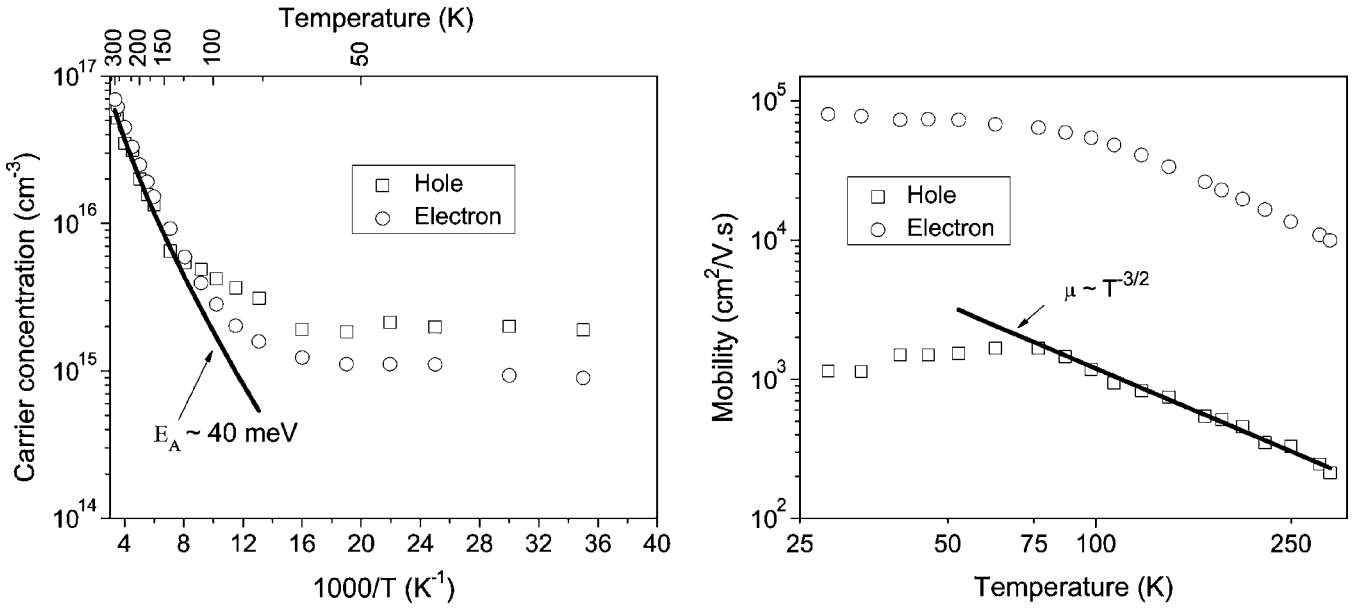

FIG. 5. Extracted carrier concentrations and temperature dependency of holes and electrons extracted for the as-grown superlattice.

spectively. Correlating the carrier concentration of both the hole and electron to the SIMS results, one can see that the hole and electron are due to the arsenic and iodine, respectively. Note that the values fall within the quoted SIMS ranges by Evans Analytical ($\pm 20\%$ for arsenic and a higher $\pm 50\%$ for iodine, due to the strong dependence on x values). At high temperatures (above 150 K), an activation energy of around 40 meV was calculated for the holes with a roll off mobility abiding to the classical $T^{-3/2}$ temperature dependence for lattice scattering.

As-grown MBE δ-doped superlattices were characterized under different conditions using x-ray diffraction, FTIR, temperature dependent Hall-effect measurements, and SIMS. Incorporated arsenic was found to be electrically active without the high temperature anneal of its alloy counterpart, thus, providing an alternative means of attaining p-type material as grown. The results from this study indicate that the δ-doping approach employed is successful in obtaining good quality low doped p-type superlattices suitable for the fabrication of photovoltaic devices used in the long wave infrared region. However, the material was observed to be highly compensated with n-type carriers that can be attributed to background impurities (iodine in this case) present in the MBE growth chamber. Further growths utilizing this method will involve higher arsenic cell temperatures to determine repeatability of the method while aiming to reduce any impurities in the growth chamber.

The authors wish to thank C. Brune for his excellent technical assistance. This work was partially funded by the Deutsche Forschungsgemeinschaft through the SFB 410 (II-VI center of excellence) at the University of Wuerzburg, the Australian Institute of Nuclear Science and Engineering (AINSE), the Australian Research Network for Advanced Materials (ARNAM), and the Australian Research Council (ARC).

[1]K. Ortner, X. C. Zhang, S. Oehling, J. Gerschutz, A. Pfeuffer-Jeschke, V. Hock, C. R. Becker, G. Landwehr, and L. W. Molenkamp, Appl. Phys. Lett. **79**, 3980 (2001).
[2]A. Rogalski, Infrared Phys. Technol. **41**, 213 (2000).
[3]H. S. Jung, P. Boieriu, and C. H. Grein, J. Electron. Mater. **35**, 1341 (2006).
[4]O. K. Wu, D. N. Jamba, and G. Sanjiv Kamath, J. Cryst. Growth **127**, 365 (1993).
[5]C. R. Becker, V. Latussek, A. Pfeuffer-Jeschke, G. Landwater, and L. W. Molenkamp, Phys. Rev. B **62**, 10353 (2000).
[6]G. K. O. Tsen, C. A. Musca, J. M. Dell, J. Antoszewski, and L. Faraone, J. Electron. Mater. **36**, 826 (2007).